HDAC1 promotes lung adenocarcinoma progression via the nuclear accumulation of β-catenin

SHIJIE XU[1,2], XIAOLU CHANG[1], XIAYU WU[3], FABAO WANG[3], JING XIANG[1], CHAOXIANG LIN[1], HE ZHAO[3], JUNZHE LI[4] and XIANHUA XU[3]

[1]Medical Research Center, Hainan Cancer Hospital, Affiliated Cancer Hospital of Hainan Medical University, Haikou, Hainan 570312, P.R. China; [2]Institute of Human Behavioral Medicine, Medical Research Center, Seoul National University, Seoul 03080, Republic of Korea; [3]Department of Pathology, Hainan Cancer Hospital, Affiliated Cancer Hospital of Hainan Medical University, Haikou, Hainan 570312, P.R. China; [4]Department of Thoracic Surgery, Hainan Cancer Hospital, Affiliated Cancer Hospital of Hainan Medical University, Haikou, Hainan 570312, P.R. China

Received May 19, 2026; Accepted July 17, 2026

DOI: 10.3892/or.2026.9175

Abstract. Histone deacetylase 1 (HDAC1) is frequently dysregulated in various human malignancies; however, the molecular mechanisms underlying its role in non-small cell lung cancer (NSCLC) remain unclear. HDAC1 expression was evaluated in 157 paired lung adenocarcinoma (LUAD) and adjacent non-neoplastic tissues using tissue microarray and immunohistochemical analysis. The functional role of HDAC1 was assessed in A549, H1299 and H1975 NSCLC cells following stable knockdown or overexpression, using Cell Counting Kit-8, colony formation and Transwell assays. Downstream signaling was examined by western blotting and nuclear-cytoplasmic fractionation. Rescue experiments were performed by overexpressing β-catenin in HDAC1-knockdown cells and the findings were further validated in a subcutaneous xenograft tumor model in nude mice. HDAC1 was markedly upregulated in LUAD tissues and associated with lymph node metastasis and poor differentiation. Functionally, HDAC1 knockdown inhibited proliferation, colony formation, migration and invasion in all three NSCLC cell lines. These effects were accompanied by downregulation of c-Myc, cyclin D1 and vimentin, upregulation of E-cadherin and reduced nuclear β-catenin accumulation. Conversely, HDAC1 overexpression enhanced malignant phenotypes and promoted β-catenin nuclear accumulation. Notably, the phosphorylation of AKT (Thr308 and Ser473) and ERK1/2 remained unaltered following HDAC1 modulation. β-catenin overexpression effectively eliminated the tumor-suppressive effects of HDAC1 knockdown both *in vitro* and *in vivo*. These findings indicated that HDAC1 is a critical promoter of LUAD progression, acting at least in part through β-catenin nuclear accumulation. This provided a mechanistic rationale for targeting the HDAC1/β-catenin axis as a potential epigenetic therapeutic strategy in LUAD.

Correspondence to: Dr Xianhua Xu, Department of Pathology, Hainan Cancer Hospital, Affiliated Cancer Hospital of Hainan Medical University, 9 Changbin West 4th Street, Xiuying, Haikou, Hainan 570312, P.R. China
E-mail: sunhwa@126.com

Dr Junzhe Li, Department of Thoracic Surgery, Hainan Cancer Hospital, Affiliated Cancer Hospital of Hainan Medical University, 9 Changbin West 4th Street, Xiuying, Haikou, Hainan 570312, P.R. China
E-mail: leeguncheol@163.com

Key words: histone deacetylase 1, lung adenocarcinoma, β-catenin, signaling pathway, molecular mechanism

Introduction

Non-small cell lung cancer (NSCLC) accounts for ~85% of all lung cancers and is a major cause of cancer-related death (1). Despite advances in diagnosis and therapy, most patients with NSCLC still present with advanced disease and overall survival remains poor (2,3). Therefore, there is an urgent need to identify novel biomarkers and therapeutic targets for NSCLC as well as to elucidate the molecular mechanisms driving its progression. Such advances would enable early detection and lead to the development of more effective treatment strategies.

Histone deacetylases (HDACs) are pivotal epigenetic regulators that catalyze the deacetylation of histones and various non-histone proteins, leading to chromatin condensation and transcriptional repression (4). A total of 18 mammalian HDACs have been identified and are classified into four groups: Class I (HDAC1, 2, 3 and 8), Class II (IIa: HDAC4, 5, 7 and 9; IIb: HDAC6 and 10), Class III (NAD^+-dependent sirtuins) and Class IV (HDAC11) (5). Among these, HDAC1 is frequently overexpressed in NSCLC (6). Elevated HDAC1 levels correlate with higher tumor grade, advanced disease stage and worse survival outcomes (7-9). HDAC1 overexpression has also been shown to enhance tumor growth, invasiveness and resistance to therapies including epidermal growth factor receptor-tyrosine kinase inhibitors and chemotherapy (10-12). However, the precise molecular mechanisms by which HDAC1 contributes to NSCLC progression remain to be fully elucidated.

HDAC1 has been implicated in multiple oncogenic signaling pathways, including the wingless-type (Wnt)/β-catenin,

phosphoinositide 3-kinase (PI3K)/protein kinase B (AKT) and mitogen-activated protein kinase (MAPK)/extracellular signal-regulated kinase (ERK) pathways. Emerging evidence indicates that HDAC1 expression is associated with activation of the PI3K/Akt and Wnt/β-catenin signaling pathways in NSCLC (13). In addition, the plant homeodomain finger protein 12-HDAC1 axis has been shown to promote EGFR/AKT signaling in NSCLC progression (14). Furthermore, the HDAC1-Smad3-mSin3A complex inhibits c-Met transcription, thereby suppressing epithelial-mesenchymal transition (EMT), angiogenesis, invasion and adhesion in lung cancer cells, which are mediated via the ERK1/2 and PI3K/Akt pathways (15). Therefore, to elucidate the mechanistic role of HDAC1 in NSCLC, the present study investigated the activities of Wnt/β-catenin, PI3K/AKT and MAPK pathways by modulating HDAC1 expression *in vitro* and *in vivo*.

Materials and methods

Patients and tissue specimens. This study was approved by the Institutional Review Committee of the Affiliated Cancer Hospital of Hainan Medical University (approval no. 2024.39). A total of 157 patients with pathologically confirmed primary lung adenocarcinoma (LUAD) who underwent surgical resection at Hainan Cancer Hospital between January 2016 and December 2024 were enrolled. The cohort comprised 69 male and 88 female patients (male-to-female ratio, 1:1.28), with a mean age of 63.1±8.5 years (range, 37-80 years). Paired tumor tissues and adjacent non-tumorous lung tissues (obtained ≥5 cm from the tumor margin) were collected at the time of surgery. Clinical and pathological data, including age at diagnosis, TNM stage (16), pathological subtype and histological grade, were retrieved from medical records. Written informed consent was obtained from all participants prior to enrollment.

Tissue microarray (TMA) construction and immunohistochemical (IHC) analyses. TMAs were constructed using paired tumor and adjacent non-tumorous tissues. Specimens were fixed in 10% neutral-buffered formalin at room temperature for 24 h, dehydrated through a graded ethanol series (50-100%; 1 h each), cleared in xylene (three changes, 30 min each), infiltrated with paraffin (three changes, 1 h each) and embedded in paraffin blocks (melting point, 58˚C). Cylindrical cores (2 mm in diameter) were extracted from representative regions of each donor block and transferred to recipient paraffin blocks using a tissue arrayer. Sections (4 μm thick) were cut from the TMA blocks, baked at 72˚C for 30 min and deparaffinized by sequential immersion in xylene (three changes) and a descending ethanol series (100, 90, 80, 70 and 50%), 5 min each. Antigen retrieval was performed in EDTA buffer (pH 9.0; cat. no. K8004; Quantum Analytics, Inc.) using an automated IHC pretreatment device at 97˚C for 18 min, followed by gradual cooling to 65˚C. Endogenous peroxidase activity was quenched with 3% hydrogen peroxide for 10 min at room temperature. The sections were then incubated with an anti-HDAC1 primary antibody (dilution, 1:100; cat. no. 34589; Cell Signaling Technology, Inc.) at room temperature for 1 h. A two-step horseradish peroxidase-conjugated detection system (cat. no. PV-9000; ZSGB-Bio, Inc.) was subsequently applied. The sections were incubated with reaction enhancement solution (Reagent 2) at room temperature for 20 min, followed by enhanced enzyme-labeled secondary antibody (Reagent 3) at 37˚C for 20 min. Immunoreactivity was visualized using 3,3'-diaminobenzidine (dilution, 1:20; cat. no. ZLI-9018; ZSGB-Bio, Inc.), and the sections were counterstained with hematoxylin at room temperature for 10-15 sec. After dehydration, clearing and mounting, images were captured under a light microscope (magnification, x40 and x400; Olympus BX53; Olympus Corporation). All slides were evaluated independently by two pathologists blinded to the clinical data.

HDAC1 expression was scored semi-quantitatively based on the staining intensity (0, negative; 1, weak; 2, moderate; 3, strong) and the proportion of positively stained cells (0, 0%; 1, <10%; 2, 10-50%; 3, 51-80%; 4, >80%). The final immunoreactive score (IRS) was calculated by multiplying the staining intensity score by the proportion score, yielding a range of 0-12. The cases were dichotomized into low-(IRS, 0-4) and high-expression (IRS, 6-12) group.

Cell culture. Human NSCLC cell lines A549, H1299 and H1975 were obtained from the Cell Bank of the Type Culture Collection of the Chinese Academy of Sciences. Cells were maintained in Roswell Park Memorial Institute-1640 (RPMI-1640) medium (cat. no. C11875500BT; Gibco; Thermo Fisher Scientific, Inc.) supplemented with 10% fetal bovine serum (FBS; cat. no. ST30-3302; PAN-Biotech GmbH) and 1% penicillin-streptomycin (cat. no. 15140-122; Gibco; Thermo Fisher Scientific, Inc.) at 37˚C in a humidified 5% CO_2 incubator.

Lentiviral packaging and stable cell line establishment. HDAC1-knockdown (HDAC1 K/D), HDAC1-overexpressing (HDAC1 O/E) and β-catenin-overexpressing (β-catenin O/E) stable cell lines were generated in A549, H1299 and H1975 cells using lentiviral transduction. For HDAC1 K/D, validated HDAC1-targeting short hairpin RNA (shRNA) sequences were cloned into the pLKO.1-GFP-puro lentiviral vector (Generay Biotech Co., Ltd.), with the empty pLKO.1 vector serving as the negative control. For HDAC1 O/E, a full-length human HDAC1 coding sequence (GenBank Accession No. NM_004964) was amplified and cloned into the pCDH-GFP-puro lentiviral vector (Generay Biotech Co., Ltd.), with the empty pCDH vector serving as the corresponding control. For β-catenin O/E, a full-length human CTNNB1 coding sequence (GenBank Accession No. NM_001904) was cloned into the same vector to generate pCDH-β-catenin, again with the empty pCDH vector as the control. The identity of each insert was verified by Sanger sequencing prior to virus production. Recombinant lentiviruses were produced using a second-generation packaging system. Briefly, 1 μg pMD2.G and 3 μg psPAX2 were cotransfected with 4 μg pCDH-HDAC1, pLKO.1-HDAC1 or pCDH-β-catenin, or with 4 μg of the corresponding empty vector (pCDH or pLKO.1), into 293T cells (cat. no. NCL-10003; NCM Biotech) using Nano293T Transfection Reagent (cat. no. C500T-1; NCM Biotech) at 37˚C for 12 h according to the manufacturer's instructions. The culture medium was replaced 12 h following transfection and virus-containing supernatants were harvested

at 24, 48 and 72 h post-transfection. The supernatants were filtered through 0.45-μm polyvinylidene fluoride membranes to remove cell debris, pooled and stored at -80˚C until use. Target cells were seeded in six-well plates and transduced with the harvested lentivirus in the presence of 8 μg/ml polybrene (MilliporeSigma). The multiplicity of infection in A549, H1299 and H1975 cells was 20, 40 and 20 for pCDH-HDAC1; 40, 40 and 20 for pLKO.1-HDAC1; and 20, 40 and 10 for pCDH-β-catenin. After 24 h, the medium was replaced with fresh complete medium. Transduced cells were selected with 6μg/ml puromycin (Beijing Solarbio Science & Technology Co., Ltd.) over 3 weeks, with the medium refreshed every 2-3 days. The resulting stable lines were designated A549-HDAC1 K/D, H1299-HDAC1 K/D and H1975-HDAC1 K/D for the knockdown groups, and A549-HDAC1 O/E, H1299-HDAC1 O/E and H1975-HDAC1 O/E for the overexpression groups, alongside their respective empty vector controls. All subsequent experiments were performed using the stable cell lines obtained after this 3-week selection period. Knockdown and overexpression efficiencies were validated by western blotting. All shRNA, overexpression and control sequences used in the present study are listed in Table SI.

To investigate whether the oncogenic effects of HDAC1 in NSCLC are mediated through β-catenin signaling, rescue experiments were performed by overexpressing β-catenin in HDAC1 K/D stable cell lines. Lentivirus production, transduction and puromycin selection were performed as described above. The resulting double-modified stable lines were designated A549-HDAC1 K/D + β-catenin O/E, H1299-HDAC1 K/D + β-catenin O/E and H1975-HDAC1 K/D + β-catenin O/E. In parallel, β-catenin was overexpressed in parental cells to generate β-catenin O/E-alone groups (A549-β-catenin O/E, H1299-β-catenin O/E and H1975-β-catenin O/E), which served as the reference groups for the rescue experiments. β-catenin overexpression efficiency was confirmed by western blotting.

Cell proliferation assay. Cell proliferation was measured using Cell Counting Kit-8 (CCK-8; Vazyme Biotech Co., Ltd.) and colony formation assays. For the CCK-8 assay, cells ($1.5x10^3$ cells/well) were seeded into 96-well plates in 200 μl culture medium. After incubation for 0, 24, 48, 72 and 96 h at 37˚C with 5% CO_2, 10 μl of CCK-8 reagent was added to each well. The absorbance was then measured at 450 nm. Cell proliferation was calculated as the optical density (OD) of the experimental well/OD of control well (Day 1). For the colony assay, cells ($1x10^4$ cells/well) were plated in 6-well plates in 2 ml complete medium and cultured for 2 weeks. The cells were fixed with 4% paraformaldehyde (MilliporeSigma) at room temperature for 30 min and stained with 0.05% crystal violet (MilliporeSigma) at room temperature for 30 min. Subsequently, colonies >1 mm in diameter were manually counted. Colony formation efficiency was calculated as the number of colonies divided by the number of cells seeded initially and the results were normalized to the control conditions. Each condition in both assays was tested in triplicate and each experiment was independently repeated at least three times.

Migration assay. Cell migration was assessed using a Transwell assay. Transwell inserts with 8-μm pore membranes (Corning Inc.) were placed in 24-well culture plates. Cells ($5x10^4$) suspended in 200 μl of serum-free culture medium were added to the upper chamber, whereas the lower chamber was filled with 600 μl of medium supplemented with 10% FBS as a chemoattractant. After 24 h of incubation at 37˚C, the non-migrated cells in the chamber were removed with a cotton swab. The migrated cells were fixed with 20% methanol for 30 min and stained with 0.1% crystal violet for 30 min (both at room temperature). Migratory cells in four randomly selected fields per insert were counted under a light microscope (magnification, x200; Olympus BX53; Olympus Corporation). Each experiment was performed in triplicate.

Invasion assay. Cell invasion was evaluated using a Matrigel-coated Transwell chamber. Transwell inserts with 8-μm pores were pre-coated with Matrigel (3 mg/ml) and the gel was allowed to solidify at 37˚C for 30 min. Then, $1x10^5$ cells suspended in 200 μl of serum-free medium were added to the upper chamber and 600 μl of medium containing 10% FBS was added to the lower chamber. After 24 h of incubation at 37˚C, non-invading cells in the upper chamber were removed with a cotton swab. The invading cells were fixed with 4% paraformaldehyde for 30 min and stained with 0.1% crystal violet for 30 min (both at room temperature). Invading cells were counted under a light microscope (magnification, x200; Olympus BX53; Olympus Corporation) across four randomly chosen fields per insert. Each experiment was performed in triplicate.

Nuclear/cytoplasmic protein separation and extraction. Nuclear and cytosolic proteins were extracted using a nucleo-cytoplasmic separation and extraction kit (Thermo Fisher Scientific Inc.) according to the manufacturer's instructions. The supernatants were collected and analyzed by western blotting. To verify the effectiveness of the fractionation, western blotting was performed using Lamin A as a nuclear marker and GAPDH as a cytoplasmic marker.

Western blotting. Cells were lysed in radioimmunoprecipitation assay buffer (Beyotime Biotechnology) containing protease inhibitors for 15 min. Lysates were clarified by centrifugation at 16,000 x g for 15 min at 4˚C. Protein concentrations were quantified using the Bradford assay (Bio-Rad Laboratories, Inc.). Samples were mixed with 5X Laemmli sample buffer and boiled. Proteins (30-40 μg/well) were separated by 8% sodium dodecyl sulfate-polyacrylamide gel electrophoresis (SDS-PAGE) and then transferred onto nitrocellulose membranes (Whatman; Cytiva). The membranes were blocked with 5% non-fat milk in Tris-buffered saline containing 0.1% Tween-20 for 1 h at room temperature, and then incubated overnight at 4˚C with primary antibodies against HDAC1 (dilution, 1:1,000), phosphorylated (p-)ERK1/2 (dilution, 1:2,000), total ERK1/2 (dilution, 1:2,000), p-AKT (T308) (dilution, 1:2,000), p-AKT (S473) (dilution, 1:2,000), total AKT (dilution, 1:2,000), c-Myc (dilution, 1:2,000), cyclin D1 (dilution, 1:2,000), E-cadherin (dilution, 1:2,000), vimentin (dilution, 1:2,000), β-catenin (dilution, 1:2,000), GAPDH (dilution, 1:3,000) and Lamin A (dilution, 1:1,000), all obtained from Cell Signaling Technology, Inc. The membranes were subsequently incubated with HRP-conjugated goat anti-rabbit

IgG (cat. no. L3012; dilution, 1:5,000; SAB Biotherapeutics, Inc.) or HRP-conjugated goat anti-mouse IgG (cat. no. L3032; dilution, 1:5,000; SAB Biotherapeutics, Inc.) for 1 h at room temperature. Signals were detected using an enhanced chemiluminescence substrate (Thermo Fisher Scientific, Inc.) and images were captured using an Amersham Imager 600 (GE Healthcare). Band intensities were quantified using ImageJ software (version 1.8.0; National Institutes of Health).

Xenograft tumor model. All animal experiments were approved by the Institutional Animal Care and Use Committee of Hainan Medical University (approval no. 2024.331) and were performed at the Medical Research Center, Hainan Cancer Hospital. A total of 20 six-week-old female BALB/c nude mice (nu/nu; body weight, 15-20 g; SJA Laboratory Animal Center) were maintained under specific pathogen-free conditions at a temperature of 22±2˚C and a relative humidity of 50±10%, with a 12-h light/dark cycle and *ad libitum* access to food and water. Prior to tumor cell inoculation, mice were allowed to acclimate for one week. A549 cells were selected as a representative lung adenocarcinoma model for the *in vivo* rescue experiments, as the *in vitro* effects of HDAC1 knockdown and β-catenin re-expression were consistent across all three cell lines (A549, H1299 and H1975). Mice were randomly divided into four groups and inoculated with stable A549 cells: empty-vector control, HDAC1 K/D, β-catenin O/E, or HDAC1 K/D + β-catenin O/E. For each mouse, $5x10^5$ cells were resuspended in 100 μl of a 1:1 mixture of PBS and Matrigel and injected subcutaneously into the right flank. Tumor diameter was measured every three days and tumor volume was calculated as (length x width^2)/2. Mice were sacrificed when any individual tumor reached ~2,000 mm^3 or when an animal lost 20% of its initial body weight, in accordance with humane endpoint guidelines. No mouse met these criteria during the study. At the experimental endpoint, four weeks after inoculation, all mice were sacrificed by carbon dioxide (CO_2) inhalation in accordance with institutional guidelines. CO_2 was introduced using a gradual-fill method at a rate displacing 30-70% of the chamber volume per minute. Tumor tissues were snap-frozen or lysed for western blotting analysis.

Statistical analyses. Data are expressed as mean ± standard deviation (SD) of at least three independent experiments. Associations between HDAC1 expression and clinicopathological characteristics were evaluated using the χ^2 test or Fisher's exact test, as appropriate. Comparisons between two groups were performed using a two-tailed Student's t-test (paired for matched tumor and adjacent tissue specimens; unpaired for independent cell-line experiments), whereas multigroup comparisons were analyzed using one-way analysis of variance followed by Tukey's post hoc test. All analyses were performed using SPSS for Windows (version 22.0; IBM Corp.). P<0.05 was considered to indicate a statistically significant difference.

Results

HDAC1 is highly expressed in LUAD. To evaluate the expression of HDAC1 in LUAD, IHC staining was performed using tissue microarrays comprising 157 paired tumor and adjacent non-neoplastic lung tissues. As shown in Fig. 1A, HDAC1 immunoreactivity was weak or absent in adjacent non-neoplastic tissues, whereas LUAD tissues exhibited strong, diffuse nuclear staining. Consistent with these observations, the mean IRS was significantly higher in LUAD tissues compared with that in the matched adjacent tissues (P<0.001; Fig. 1B). When cases were dichotomized by IRS, high HDAC1 expression was detected in 143 of 157 (91.1%) LUAD specimens, compared with only 37 of 157 (23.6%) adjacent non-neoplastic tissues (χ^2=146.273, P<0.001; Table I). These results demonstrated that HDAC1 is frequently overexpressed in LUAD.

HDAC1 expression is associated with clinicopathological features of LUAD patients. The association between HDAC1 expression and the clinicopathological characteristics was further analyzed (Table II). High HDAC1 expression was significantly associated with lymph node metastasis (P=0.027) and the histological differentiation grade (P=0.006). Notably, all 46 patients with lymph node metastasis (100%) exhibited high HDAC1 expression compared with 97 of 111 (87.4%) patients without lymph node involvement. Regarding tumor differentiation, the proportion of high HDAC1 expression was greatest in poorly differentiated tumors (64/65, 98.5%), followed by well to moderately differentiated tumors (79/92, 85.9%), suggesting that HDAC1 upregulation is accompanied by a less differentiated and more aggressive phenotype. By contrast, no significant association was observed between HDAC1 expression and patient age, sex, maximum tumor diameter, T stage, vascular invasion, perineural invasion, necrotic components, or Ki-67 proliferation index (all P>0.05). Collectively, these findings indicate that elevated HDAC1 expression is closely linked to lymph node metastasis and poor tumor differentiation in LUAD.

HDAC1 K/D suppresses proliferation, migration and invasion while reducing nuclear β-catenin accumulation in NSCLC cells. To examine the functional role of HDAC1 in NSCLC, the present study established stable HDAC1-K/D cell lines using two independent shRNA constructs (K/D-1 and K/D-2) in A549, H1299 and H1975 cells. CCK-8 assay revealed that HDAC1 knockdown significantly reduced the proliferative capacity of all three cell lines over a 96-h observation period compared with the empty vector controls (P<0.001; Fig. 2A-C). Colony formation assays further confirmed these findings; HDAC1-K/D cells exhibited significantly reduced clonogenic ability compared with control cells (P<0.001; Fig. 2D and E). Next, it was examined whether HDAC1 depletion affects the migratory and invasive potential of NSCLC cells using Transwell assays. HDAC1 knockdown led to a significant reduction in both the migration (Fig. 2F and G) and invasiveness (Fig. 2H and I) of all three cell lines relative to their respective controls (P<0.001). Collectively, these data indicated that HDAC1 is required for the proliferative, migratory and invasive capacities of NSCLC cells.

Previous studies have demonstrated that HDAC1 expression is associated with activation of the PI3K/Akt, MAPK/ERK and Wnt/β-catenin signaling pathways in lung cancer (13-15). To determine which of these pathways mediated the observed phenotypes, the present study examined

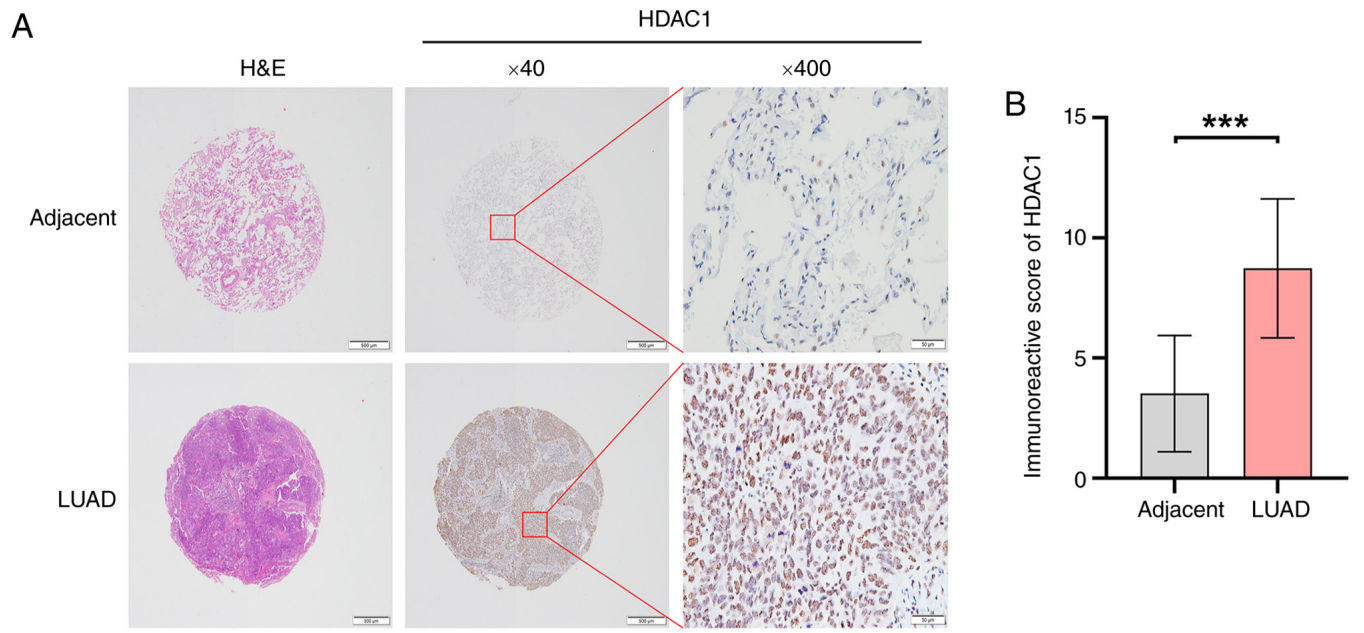

Figure 1. HDAC1 expression in LUAD and adjacent non-neoplastic tissues. (A) Representative H&E staining (left panels; magnification, x40) and immunohistochemical staining for HDAC1 (middle and right panels) in adjacent non-neoplastic lung tissues (upper row) and LUAD tissues (lower row) from tissue microarray sections. HDAC1 immunostaining is shown at x40 magnification (middle panels) with corresponding higher-magnification views at x400 (right panels). (B) Quantification of the IRS for HDAC1 in paired adjacent non-neoplastic and LUAD tissues (n=157 pairs). Data are presented as mean ± SD and were analyzed using two-tailed paired Student's t-test. ***P<0.001. HDAC1, histone deacetylase 1; LUAD, lung adenocarcinoma; H&E, hematoxylin and eosin; IRS, immunoreactive score.

the expression of key signaling molecules by western blotting and nuclear-cytoplasmic fractionation (Fig. 2J-M). HDAC1 K/D significantly decreased c-Myc and cyclin D1 protein levels in all three cell lines (P<0.05), indicating impaired cell cycle progression following HDAC1 depletion. With respect to EMT markers, HDAC1 silencing led to a marked increase in the epithelial marker E-cadherin (P<0.01) and a concomitant decrease in the mesenchymal marker vimentin (P<0.01), indicating a reversal of the mesenchymal phenotype. Subcellular fractionation analysis further revealed that nuclear β-catenin levels were substantially reduced in HDAC1-K/D cells (P<0.001), whereas cytoplasmic β-catenin remained largely unchanged (P>0.05), suggesting that HDAC1 promoted the nuclear accumulation of β-catenin. By contrast, the phosphorylation of AKT (at both Thr308 and Ser473) and ERK as well as the total AKT and ERK protein levels showed no significant alterations following HDAC1 knockdown (P>0.05), indicating that the PI3K/AKT and MAPK/ERK pathways are not the primary downstream effectors of HDAC1 in this context. Thus, these results demonstrated that HDAC1 knockdown suppresses the proliferation, migration and invasion of NSCLC cells, accompanied by downregulation of c-Myc and cyclin D1, reversal of EMT and reduced nuclear accumulation of β-catenin.

HDAC1 O/E promotes proliferation, migration and invasion and enhances nuclear β-catenin accumulation in NSCLC cells. The present study performed reciprocal gain-of-function experiments by stably overexpressing HDAC1 in A549, H1299 and H1975 cells. CCK-8 assays demonstrated that HDAC1 O/E significantly enhanced the proliferative capacity of all three cell lines over a 96-h period compared with the empty-vector controls (P<0.001; Fig. 3A-C). Consistent with these results, colony formation assays revealed that HDAC1-O/E cells exhibited significantly greater clonogenic ability than the control cells (P<0.001; Fig. 3D and E). Transwell assays further showed that HDAC1 O/E augmented both the migratory (Fig. 3F and G) and invasive (Fig. 3H and I) abilities of all three cell lines (P<0.001 for all comparisons). These gain-of-function data mirror the knockdown results and collectively established that HDAC1 promotes the proliferation, migration and invasion of NSCLC cells.

Next, the present study assessed the effect of HDAC1 O/E on downstream signaling molecules using western blotting and nuclear-cytoplasmic fractionation (Fig. 3J-M). Consistent with the knockdown data, HDAC1 O/E led to significant upregulation of c-Myc (P<0.01) and cyclin D1 (P<0.01) protein levels across all three cell lines, further supporting the role of HDAC1 in driving cell cycle progression. Regarding EMT-related markers, HDAC1 O/E resulted in a marked decrease in E-cadherin expression (P<0.01) and a corresponding increase in vimentin expression (P<0.01), indicating a shift toward a mesenchymal phenotype. Subcellular fractionation analysis demonstrated that nuclear β-catenin levels were substantially elevated in HDAC1-O/E cells (P<0.001), whereas cytoplasmic β-catenin remained largely unchanged (P>0.05), reinforcing the idea that HDAC1 facilitates nuclear accumulation of β-catenin. Consistent with the knockdown data, neither the phosphorylation of AKT (Thr308 and Ser473) nor ERK or total AKT and ERK protein levels were significantly affected by HDAC1 O/E (P>0.05 for all comparisons). Collectively, the complementary knockdown and overexpression results demonstrated that HDAC1 drives NSCLC cell proliferation, migration and invasion, at least in part through upregulation of c-Myc and cyclin D1, induction of

Table I. Expression of HDAC1 in lung adenocarcinoma tissues and adjacent non-neoplastic tissues (n=157).

HDAC1 IHC score	Lung adenocarcinoma tissues n (%)	Adjacent non-neoplastic tissues n (%)	χ^2	P-value
High	143 (91.1)	37 (23.6)	146.273	<0.001
Low	14 (8.9)	120 (76.4)		

HDAC1, histone deacetylase 1; IHC, immunohistochemical.

Table II. Relationship between HDAC1 expression and clinicopathological features (n=157).

	HDAC1 Expression			
Clinicopathological features	High, n (%)	Low, n (%)	Total	P-value
Age (years)				0.220
≤60	43 (86.0)	7 (14.0)	50	
>60	100 (93.5)	7 (6.5)	107	
Sex				0.515
Male	64 (92.8)	5 (7.2)	69	
Female	79 (89.8)	9 (10.2)	88	
Maximum tumor diameter (mm)				1.000
≤30	110 (90.9)	11 (9.1)	121	
>30	33 (91.7)	3 (8.3)	36	
T stage				0.375
T1	64 (88.9)	8 (11.1)	72	
T2-T4	79 (92.9)	6 (7.1)	85	
Lymph node metastasis				0.027[a]
Yes	46 (100.0)	0 (0.0)	46	
No	97 (87.4)	14 (12.6)	111	
Vascular invasion				0.461
Yes	39 (95.1)	2 (4.9)	41	
No	104 (89.7)	12 (10.3)	116	
Perineural invasion				1.000
Yes	9 (90.0)	1 (10.0)	10	
No	134 (91.2)	13 (8.8)	147	
Necrotic component				0.577
Yes	24 (96.0)	1 (4.0)	25	
No	119 (90.2)	13 (9.8)	132	
Degree of differentiation				0.006[b]
Well-Moderate	79 (85.9)	13 (14.1)	92	
Poor	64 (98.5)	1 (1.5)	65	
Ki-67				0.531
≤10%	95 (89.6)	11 (10.4)	106	
>10%	48 (94.1)	3 (5.9)	51	

[a]P<0.05, [b]P<0.01. HDAC1, histone deacetylase 1

EMT and promotion of nuclear β-catenin accumulation, independent of the PI3K/AKT and MAPK/ERK pathways.

β-catenin O/E reverses the tumor-suppressive effects of HDAC1 K/D in NSCLC cells. To determine whether β-catenin signaling is functionally required for HDAC1-mediated oncogenic effects, the present study overexpressed β-catenin in HDAC1-K/D A549, H1299 and H1975 cells. Four experimental groups were established: Empty-vector control, HDAC1 K/D alone, β-catenin O/E alone and HDAC1 K/D + β-catenin O/E.

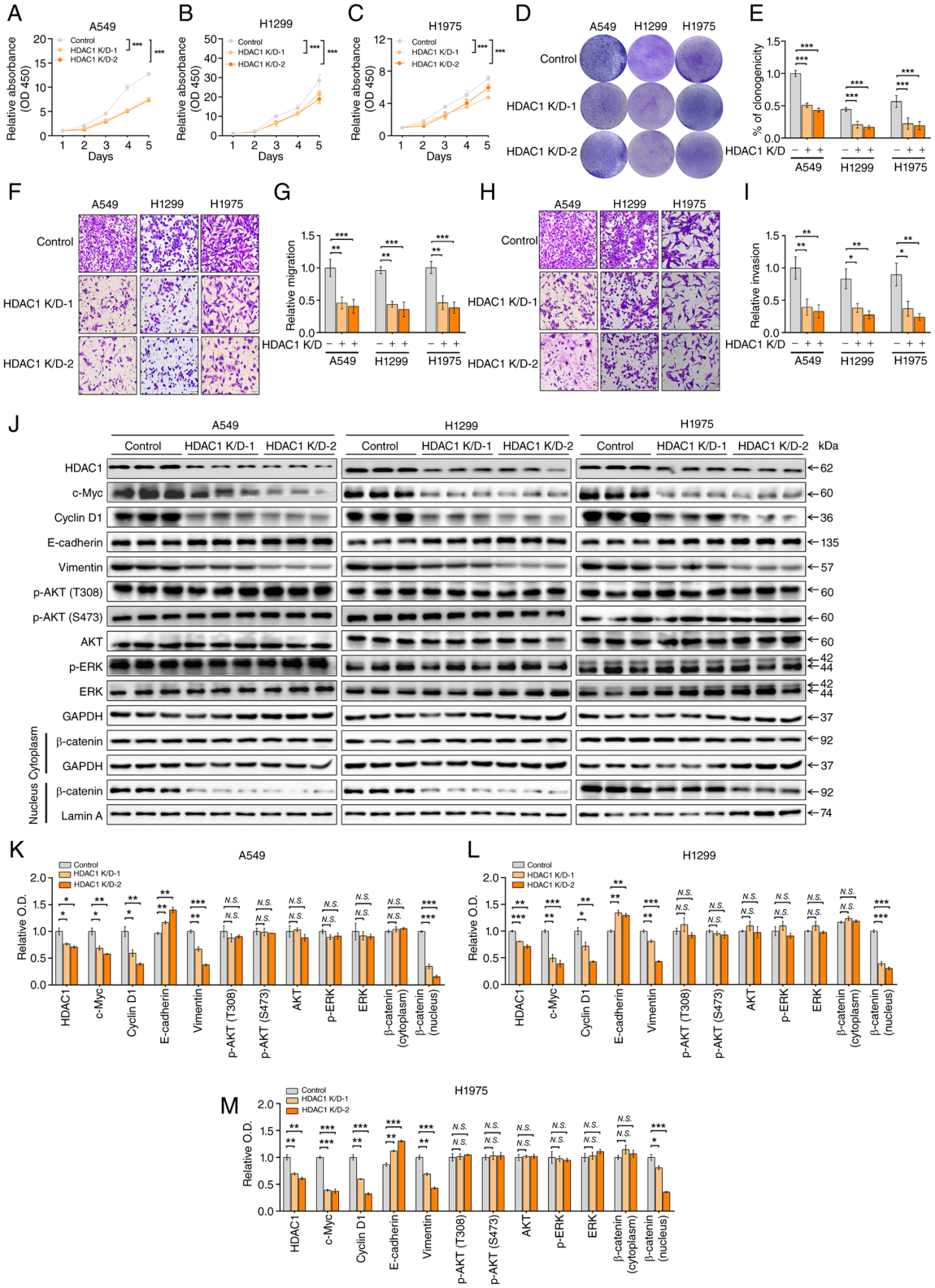

Figure 2. Effects of HDAC1 knockdown on proliferation, migration, invasion and downstream signaling in NSCLC cells. A549, H1299 and H1975 cells were stably transduced with HDAC1-targeting shRNA (K/D-1 and K/D-2) or empty vector (Control). Cell proliferation was measured using CCK-8 assay over a 96-h period in (A) A549, (B) H1299 and (C) H1975 cells. (D) Representative images of colony formation assays in A549, H1299 and H1975 cells. (E) Quantification of clonogenicity from colony formation assays. (F) Representative images of Transwell migration assays in A549, H1299 and H1975 cells. Crystal violet staining; original magnification, x200. (G) Quantification of relative migration. (H) Representative images of Transwell invasion assays performed using Matrigel-coated chambers. Crystal violet staining; original magnification, x200. (I) Quantification of relative invasion. (J) Western blotting of HDAC1, c-Myc, cyclin D1, E-cadherin, vimentin, p-AKT (Thr308), p-AKT (Ser473), total AKT, p-ERK and total ERK in whole-cell lysates and β-catenin in cytoplasmic and nuclear fractions of A549, H1299 and H1975 cells. GAPDH and Lamin A served as loading controls for whole cell/cytoplasmic and nuclear fractions, respectively. Densitometric quantification of protein levels normalized to the respective loading controls in (K) A549, (L) H1299 and (M) H1975 cells. Data are presented as mean ± SD from three independent experiments and were analyzed using two-tailed unpaired Student's t-test. *P<0.05, **P<0.01 and ***P<0.001. N.S., not significant; HDAC1, histone deacetylase 1; NSCLC, non-small cell lung cancer; sh, short hairpin; CCK-8, Cell Counting Kit-8; p-, phosphorylated; AKT, protein kinase B; ERK, extracellular signal-regulated kinase.

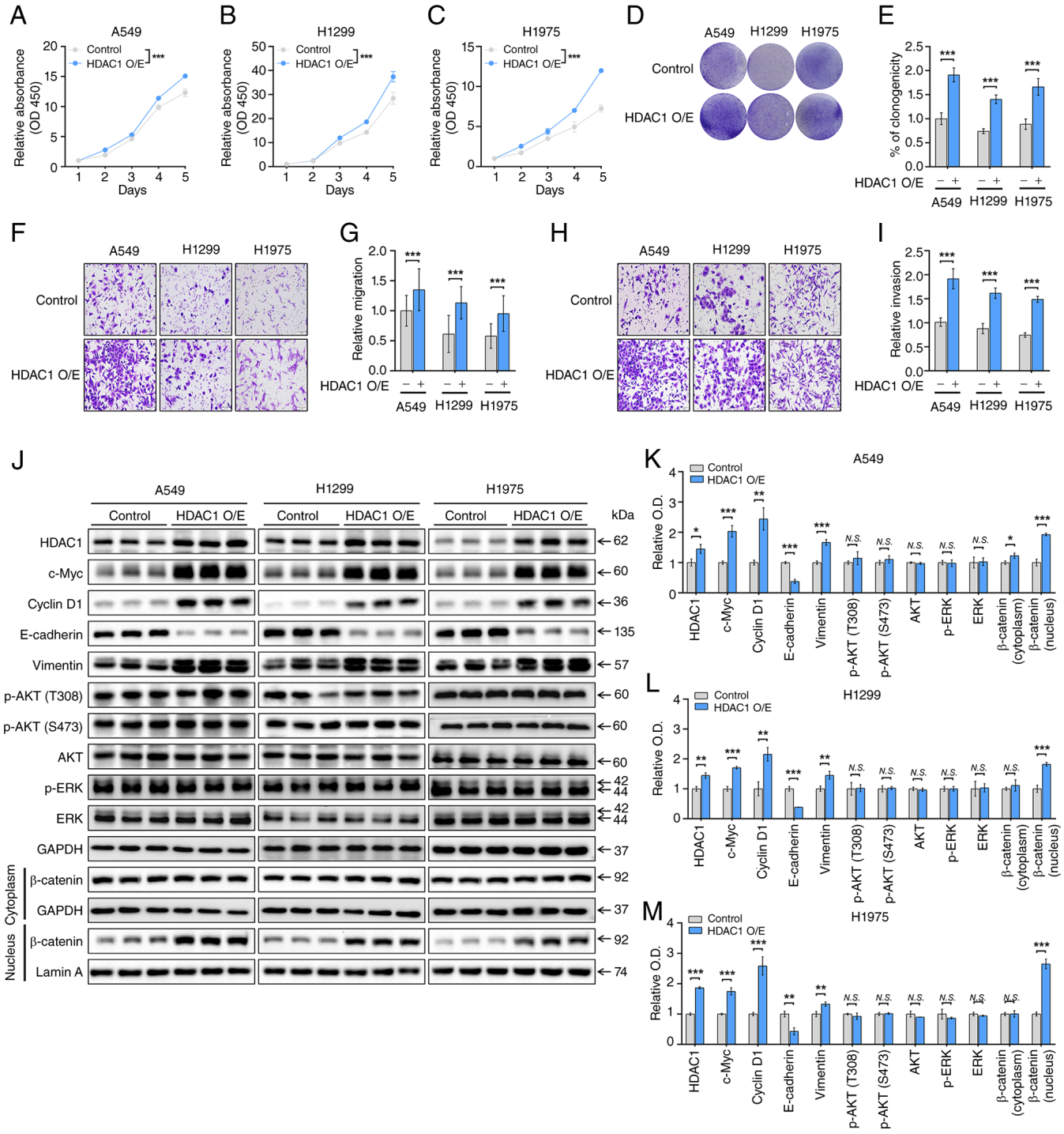

Figure 3. Effects of HDAC1 overexpression on proliferation, migration, invasion and downstream signaling in NSCLC cells. A549, H1299 and H1975 cells were stably transduced with HDAC1-overexpressing lentivirus (HDAC1 O/E) or empty vector (Control). Cell proliferation was measured using CCK-8 assay over a 96-h period in (A) A549, (B) H1299 and (C) H1975 cells. (D) Representative images of colony formation assays in A549, H1299 and H1975 cells. (E) Quantification of clonogenicity from colony formation assays. (F) Representative images of Transwell migration assays in A549, H1299 and H1975 cells. Crystal violet staining; original magnification, x200. (G) Quantification of relative migration. (H) Representative images of Transwell invasion assays performed using Matrigel-coated chambers. Crystal violet staining; original magnification, x200. (I) Quantification of relative invasion. (J) Western blotting of HDAC1, c-Myc, cyclin D1, E-cadherin, vimentin, p-AKT (Thr308), p-AKT (Ser473), total AKT, p-ERK and total ERK in whole-cell lysates and β-catenin in cytoplasmic and nuclear fractions of A549, H1299 and H1975 cells. GAPDH and Lamin A served as loading controls for whole cell/cytoplasmic and nuclear fractions, respectively. Densitometric quantification of protein levels normalized to the respective loading controls in (K) A549, (L) H1299 and (M) H1975 cells. Data are presented as mean ± SD from three independent experiments and were analyzed using two-tailed unpaired Student's t-test. *P<0.05, **P<0.01 and ***P<0.001. N.S., not significant; HDAC1, histone deacetylase 1; NSCLC, non-small cell lung cancer; O/E, overexpressing.

As shown in Fig. 4A-C, CCK-8 assays revealed that HDAC1 K/D alone significantly suppressed the proliferative capacity of all three cell lines (P<0.001), whereas β-catenin O/E alone enhanced cell proliferation (P<0.001). Notably, co-expression of β-catenin in HDAC1-K/D cells restored proliferation to levels comparable to those of the β-catenin O/E group (P>0.05,

HDAC1 K/D + β-catenin O/E vs. β-catenin O/E), indicating that β-catenin overexpression effectively abrogates the growth-inhibitory effect of HDAC1 silencing. Colony formation assays yielded concordant results; the reduced clonogenic ability caused by HDAC1 knockdown was effectively rescued by concomitant β-catenin overexpression (P>0.05, HDAC1 K/D + β-catenin O/E vs. β-catenin O/E; Fig. 4D and E). Similarly, Transwell assays demonstrated that β-catenin O/E largely reversed the inhibitory effects of HDAC1 K/D on both migration (P>0.05; Fig. 4F and G) and invasion (P>0.05; Fig. 4H and I) in all three cell lines. The double-modified group showed no significant difference compared with the β-catenin O/E-alone group for either endpoint. These results indicated that HDAC1 promotes NSCLC cell proliferation, migration and invasion, at least in part through β-catenin signaling.

Western blotting and nuclear-cytoplasmic fractionation further corroborated these functional observations at the molecular level (Fig. 4J-M). Consistent with earlier findings, HDAC1 K/D alone reduced c-Myc, cyclin D1 and vimentin protein levels while upregulating E-cadherin. Simultaneous overexpression of β-catenin in HDAC1-K/D cells effectively reversed these molecular changes: c-Myc, cyclin D1 and vimentin levels were restored and E-cadherin was suppressed to levels comparable with that of the β-catenin O/E-alone group (P>0.05, HDAC1 K/D + β-catenin O/E vs. β-catenin O/E). Subcellular fractionation revealed that nuclear β-catenin level, which was reduced following HDAC1 K/D (P<0.01), was substantially restored following β-catenin O/E (P>0.05), whereas cytoplasmic β-catenin levels remained relatively stable across all groups (P>0.05). Taken together, these results demonstrated that β-catenin functions as a critical downstream effector of HDAC1 in NSCLC cells. The tumor-promoting activities of HDAC1, including enhanced proliferation, migration, invasion and EMT, are largely dependent on β-catenin nuclear accumulation and its downstream transcriptional activity.

β-catenin O/E inhibits HDAC1 K/D-mediated tumor growth inhibition in a xenograft tumor model. To validate the proposed molecular mechanism *in vivo*, the present study established a subcutaneous xenograft tumor model. A549 cells stably expressing empty vector (control), HDAC1 K/D, β-catenin O/E, or HDAC1 K/D + β-catenin O/E were injected subcutaneously into the flanks of nude mice (n=5 per group; Fig. 5A) and tumor growth was monitored over a 28-day period. HDAC1 K/D significantly suppressed xenograft tumor growth; both the final tumor volume and tumor weight in the HDAC1 K/D group were significantly reduced compared with those in the control group (P<0.001; Fig. 5B-D). Conversely, β-catenin O/E alone yielded significantly larger and heavier tumors than controls (P<0.001). Critically, simultaneous overexpression of β-catenin in HDAC1-K/D cells restored tumor volume and weight to levels comparable to those in the control group (P>0.05, HDAC1 K/D + β-catenin O/E vs. control; Fig. 5C-E), effectively abolishing the growth-inhibitory effect of HDAC1 silencing. Body weight remained stable in all four groups throughout the experimental period, indicating no overt systemic toxicity (Fig. 5F).

To determine whether the molecular changes observed *in vitro* are recapitulated *in vivo*, the present study performed western blotting of harvested tumor tissues (Fig. 5G and H). HDAC1 K/D reduced c-Myc, cyclin D1 and vimentin protein levels (P<0.01) and upregulated E-cadherin expression in xenograft tissues (P<0.01), which was consistent with the *in vitro* data. Importantly, concomitant β-catenin O/E in HDAC1-K/D cells effectively reversed these alterations: c-Myc, cyclin D1 and vimentin levels were restored and E-cadherin was suppressed to levels comparable to those in the β-catenin O/E-alone group (P>0.05, HDAC1 K/D + β-catenin O/E vs. β-catenin O/E). Subcellular fractionation of tumor lysates demonstrated that nuclear β-catenin, which was reduced following HDAC1 K/D (P<0.01), was substantially restored following β-catenin O/E (P>0.05, HDAC1 K/D + β-catenin O/E vs. β-catenin O/E), whereas cytoplasmic β-catenin levels remained relatively stable across all groups (P>0.05). Notably, β-catenin O/E did not alter HDAC1 protein levels (P>0.05), confirming that the observed rescue effect was mediated by β-catenin reactivation rather than by restoration of HDAC1 expression. In summary, these *in vivo* data are in full agreement with the *in vitro* observations and provide compelling evidence that HDAC1 promotes LUAD tumorigenesis through a β-catenin-dependent mechanism.

Discussion

The main purpose of the present study was to elucidate the molecular mechanisms by which HDAC1 influences LUAD progression. The present study found that inhibition of HDAC1 markedly reduced nuclear β-catenin levels, whereas HDAC1 O/E produced the opposite effect, increasing nuclear β-catenin accumulation. In addition, the β-catenin O/E blocked the tumor-suppressive effect of HDAC1 inhibition in NSCLC, both *in vitro* and *in vivo*. These findings indicate that HDAC1 promotes LUAD tumorigenesis, at least in part, through modulation of the β-catenin signaling pathway. HDAC1 functions primarily as a transcriptional repressor. It has also been reported to interact directly with β-catenin and to catalyze deacetylation that triggers ubiquitin-mediated degradation (17,18). On the basis of this mechanism, HDAC1 inhibition would be expected to stabilize β-catenin, promote its nuclear accumulation (19) and thereby enhance transcription of proliferation-related genes such as c-Myc and cyclin D1 (20-22). The present data showed the opposite relationship in LUAD, indicating that the effect of HDAC1 on β-catenin is context-dependent. One explanation is that HDAC1 overexpression selectively silences negative regulators of the Wnt/β-catenin pathway, thereby relieving inhibition of β-catenin signaling. Consistent with this possibility, HDAC inhibitor treatment increased histone H3 acetylation at the promoters of the Wnt/β-catenin repressors DKK1, SFRP1 and WIF1 and restored their expression (23). HDAC1 inhibition may thus reactivate tumor suppressor genes and attenuate tumor progression (24). Elevated HDAC1 levels in LUAD may therefore drive aberrant Wnt/β-catenin signaling through epigenetic silencing of endogenous β-catenin inhibitors.

HDAC1 modulation altered the nuclear pool of β-catenin without affecting the cytoplasmic pool, a pattern consistent with the compartmentalized regulation of this protein. Within the cell, β-catenin is distributed across three distinct pools: Membranous, cytoplasmic and nuclear (25-27). The nuclear

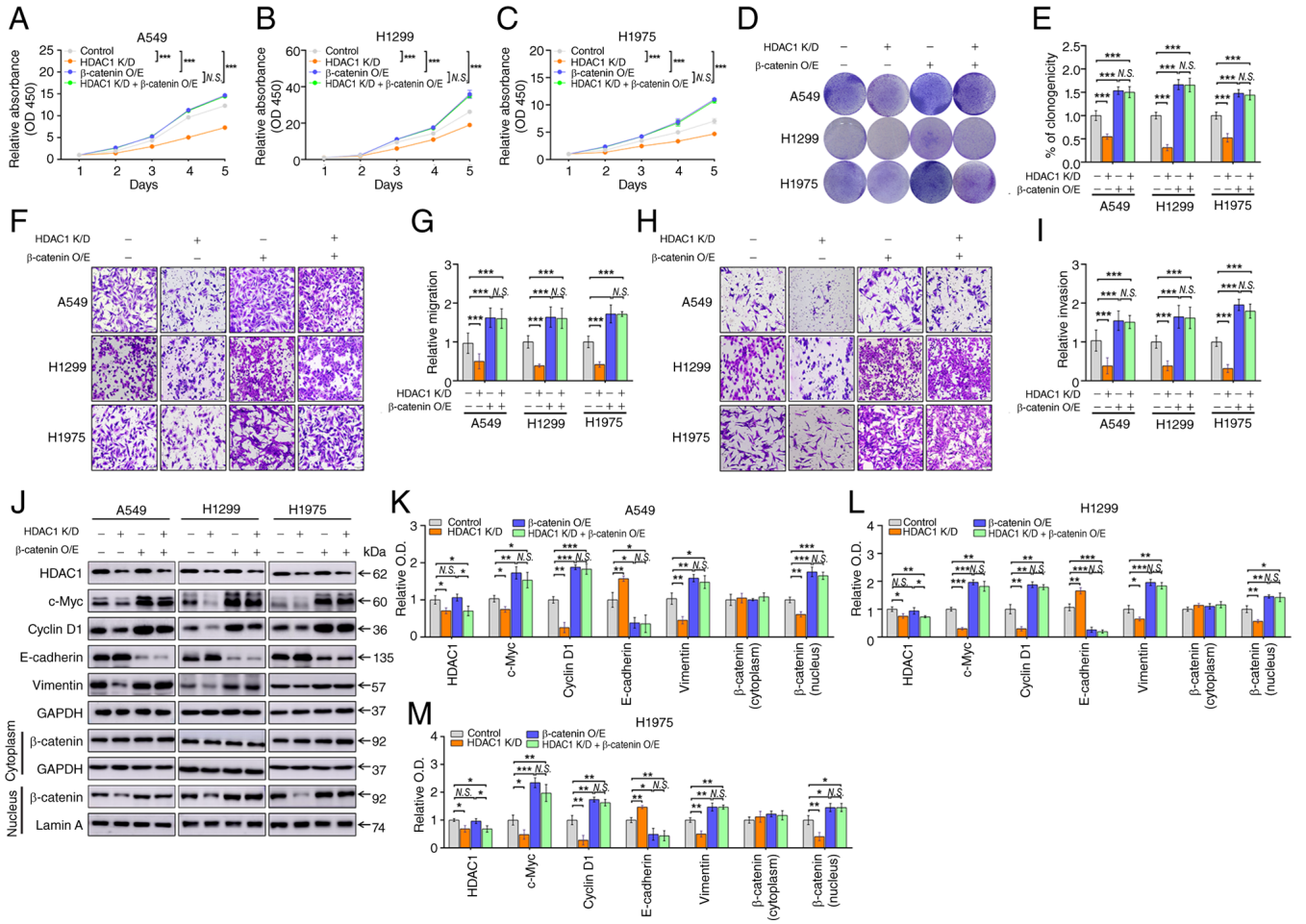

Figure 4. Effects of combined HDAC1 knockdown and β-catenin overexpression on malignant phenotypes and downstream signaling in NSCLC cells. A549, H1299 and H1975 cells were stably transduced to generate four experimental groups: empty-vector control, HDAC1 K/D, β-catenin O/E and HDAC1 K/D + β-catenin O/E. (A-C) Cell proliferation was measured using CCK-8 assay over a 96-h period in (A) A549, (B) H1299 and (C) H1975 cells. (D) Representative images of colony formation assays in A549, H1299 and H1975 cells. (E) Quantification of clonogenicity from colony formation assays. (F) Representative images of Transwell migration assays in A549, H1299 and H1975 cells. Crystal violet staining; original magnification, x200. (G) Quantification of relative migration. (H) Representative images of Transwell invasion assays performed using Matrigel-coated chambers. Crystal violet staining; original magnification, x200. (I) Quantification of relative invasion. (J) Western blotting of HDAC1, c-Myc, cyclin D1, E-cadherin and vimentin in whole-cell lysates and β-catenin in cytoplasmic and nuclear fractions of A549, H1299 and H1975 cells. GAPDH and Lamin A served as loading controls for whole cell/cytoplasmic and nuclear fractions, respectively. (K-M) Densitometric quantification of protein levels normalized to the respective loading controls in (K) A549, (L) H1299 and (M) H1975 cells. Data are presented as mean ± SD from three independent experiments and were analyzed using one-way ANOVA followed by Tukey's post hoc test. *P<0.05, **P<0.01 and ***P<0.001. N.S., not significant; HDAC1, histone deacetylase 1; NSCLC, non-small cell lung cancer; K/D, knockdown; O/E, overexpression.

pool constitutes only a minor fraction of the total protein (28). A change large enough to alter nuclear levels may therefore produce only a small, statistically undetectable shift in the much larger cytoplasmic pool. Importantly, the transcriptional activity of β-catenin depends on the nuclear fraction and its binding to TCF/LEF factors rather than on total abundance (29). Thus, these findings indicated that HDAC1 acts principally on the nuclear accumulation and transcriptional activity of β-catenin. The stability of the cytoplasmic pool favors this interpretation over a degradation-based mechanism, although altered β-catenin stability cannot be entirely excluded.

The AKT and ERK signaling cascades serve as critical regulators of proliferation and survival in NSCLC cells (30-32). A previous study demonstrated that the HDAC1-Smad3-mSin3A transcriptional complex coordinately suppresses c-Met expression, subsequently reducing phosphorylation of both ERK and AKT, while simultaneously inhibiting EMT and invasion in lung cancer (15); HDAC1 activity was associated with reduced phosphorylation of AKT and ERK1/2. However, in the present study, altering HDAC1 expression did not markedly affect the phosphorylation of either kinase in NSCLC cells. This discrepancy likely stems from key methodological differences between the studies. Previous work has suggested that Smad3, rather than HDAC1, directly mediates AKT/ERK regulation, implying that Smad3 may engage in alternative mechanisms independent of HDAC1 (15). Accumulating evidence indicates that Smad3 confers radiotherapy resistance in NSCLC cells through the ITGA6/PI3K/AKT axis (33). Furthermore, phosphorylated ERK directly interacts with and modulates Smad3 function (34). Thus, the present study indicated that HDAC1 does not independently regulate AKT or ERK1/2 activity in NSCLC cell lines, highlighting the inherent complexity of these signaling networks and underscoring the importance

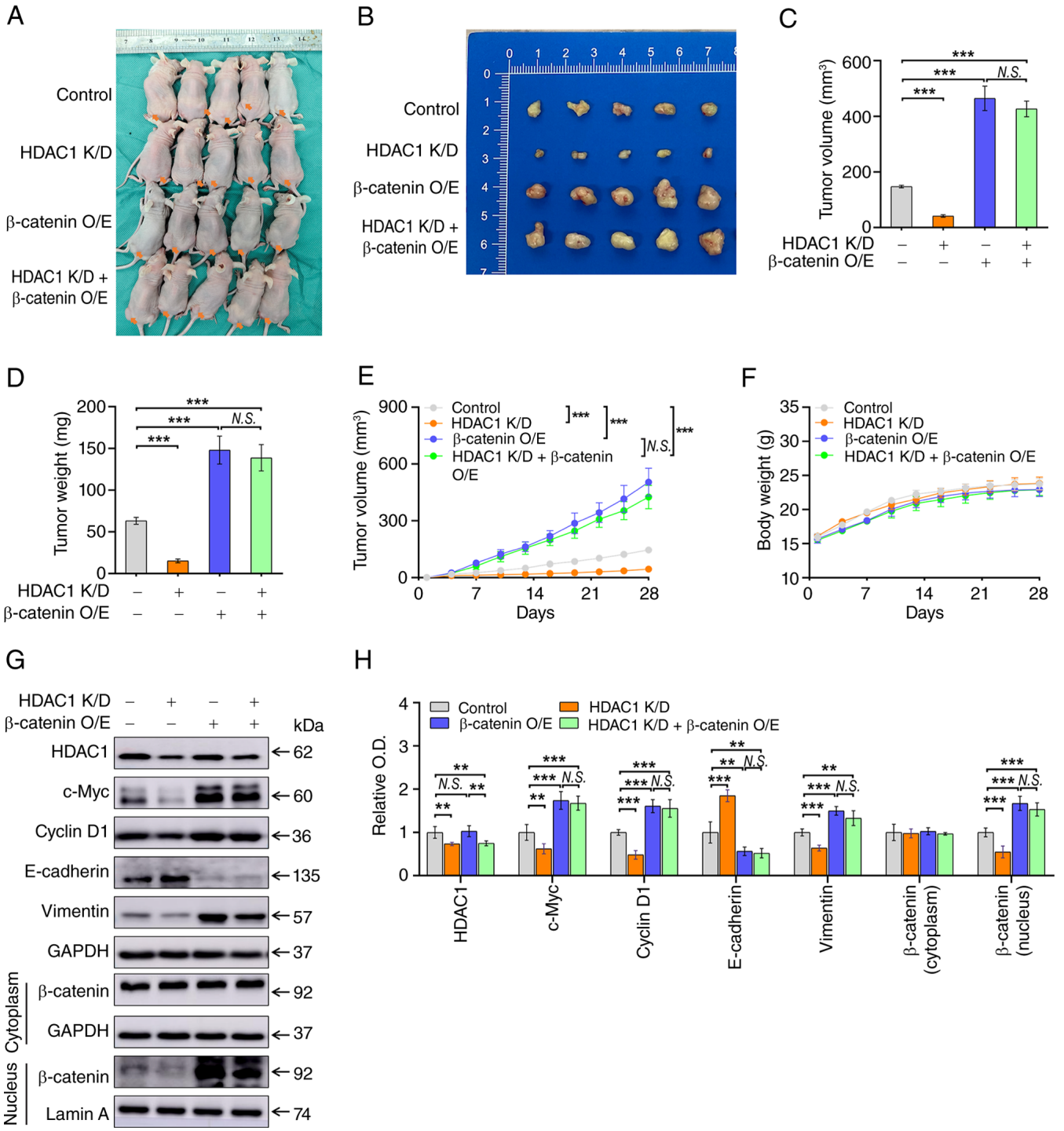

Figure 5. *In vivo* effects of combined HDAC1 knockdown and β-catenin overexpression on tumor growth and downstream signaling in a xenograft tumor model. A549 cells stably expressing empty vector (Control), HDAC1 K/D, β-catenin O/E, or HDAC1 K/D + β-catenin O/E were injected subcutaneously into the flanks of BALB/c nude mice (n=5 per group). (A) Representative image of tumor-bearing mice at the experimental endpoint (day 28). (B) Gross appearance of excised tumors from each group. (C) Final tumor volume (mm^3) and (D) Final tumor weight (mg) at the experimental endpoint. (E) Tumor growth curves measured over a 28-day observation period. Tumor volume was calculated using the formula V=0.5 x length x $width^2$. (F) Body weight of mice was monitored over the 28-day experimental period. (G) Western blotting of HDAC1, c-Myc, cyclin D1, E-cadherin and vimentin in whole-cell lysates and β-catenin in cytoplasmic and nuclear fractions of harvested tumor tissues. GAPDH and Lamin A served as loading controls for whole cell/cytoplasmic and nuclear fractions, respectively. (H) Densitometric quantification of protein levels normalized to the respective loading controls. Data are presented as mean ± SD (n=5 per group) and were analyzed using one-way ANOVA followed by Tukey's post hoc test. $^{**}P<0.01$, $^{***}P<0.001$. N.S., not significant; HDAC1, histone deacetylase 1.

of examining multiple regulatory nodes when identifying therapeutic targets (11,12,35).

HDAC1 overexpression is associated with tumor progression and poor prognosis in gastric cancer (36,37), colorectal cancer (38,39) and LUAD (9). A meta-analysis further confirmed that HDAC1 expression was associated with the histological differentiation grade and worse overall survival in lung cancer, although its association with lymph node

metastasis remains inconclusive (8). In the present study, HDAC1 protein was highly expressed in 91.1% of the LUAD tissues and was significantly associated with poor histological differentiation (P=0.006) and lymph node metastasis (P=0.027). Enrichment of HDAC1 in poorly differentiated tumors is biologically plausible because HDAC1 is specifically overexpressed in cancer stem cells and is essential for maintaining stem cell properties (40). Mechanistically, HDAC1 promotes cellular dedifferentiation by forming transcriptional repressor complexes that silence the differentiation-associated genes via histone deacetylation (41,42). Furthermore, the association between HDAC1 and lymph node metastasis is consistent with the functional data of the present study showing that HDAC1 drives EMT, enhances migratory and invasive capacity and promotes nuclear β-catenin accumulation. Collectively, these findings supported HDAC1 as both a functional driver of aggressive LUAD behavior and a potential biomarker for identifying high-risk patients.

The present study has several limitations. First, although survival data would further strengthen the clinical significance of the findings, a reliable survival analysis was not feasible in the present cohort. The low-HDAC1 expression group was small (n=14), the follow-up was relatively short and no mortality occurred in this group. Consequently, no significant difference in survival was detected between the high- and low-expression groups. This imbalance reflects the high prevalence of HDAC1 expression in lung adenocarcinoma, which leaves few low-expression cases for comparison, rather than indicating a sampling bias. Future studies are needed to clarify the prognostic value of HDAC1 in larger cohorts with longer follow-up. Second, only the PI3K/AKT and MAPK/ERK pathways were examined alongside Wnt/β-catenin. Other HDAC1-regulated pathways that may contribute to tumor progression were not assessed. The present study therefore established β-catenin as a necessary downstream effector without excluding additional mechanisms.

In conclusion, the present study demonstrated that HDAC1 inhibition markedly suppressed the proliferation, migration and invasion of NSCLC cells, accompanied by reduced nuclear β-catenin levels. Conversely, HDAC1 overexpression promoted these malignant behaviors by enhancing β-catenin nuclear localization. Moreover, restoration of β-catenin expression effectively abolished the anti-tumor effects of HDAC1 inhibition both *in vitro* and *in vivo*, indicating that HDAC1 promotes LUAD progression, at least in part, through β-catenin signaling. Furthermore, HDAC1-mediated regulation occurred independently of the major proliferative pathways, as neither AKT nor ERK1/2 phosphorylation was affected by HDAC1 modulation alone. These findings provided a strong rationale for developing HDAC1 inhibitor-based therapeutic strategies for LUAD.

Acknowledgments

Not applicable.

Funding

The present study was supported by the Nanhai Xinxing project of Hainan Province (grant no. NHXXRCXM202350) and the National Natural Science Foundation of China (grant nos. 82460608 and 82260275). Support was also provided by the Joint Program on Health Science & Technology Innovation of Hainan Province (grant nos. WSJK2026MS254 and WSJK2026QN184).

Availability of data and materials

The data generated in the present study may be requested from the corresponding author.

Authors' contributions

SX and XX designed the study and acquired funding. SX, XC, FW, JX and CL performed the experiments and analyzed the data. XW and HZ collected the clinical samples and provided materials. JL provided materials and supervised the study. SX drafted the manuscript. JL and XX reviewed and edited the manuscript. SX, JL and XX confirm the authenticity of all the raw data. All authors read and approved the final manuscript.

Ethics approval and consent to participate

The animal study was approved by Institutional Animal Care and Use Committee (IACUC) at Hainan Medical University (approval no. 2024.331). Human subject studies were approved by the Institutional Review Committee of the Affiliated Cancer Hospital of Hainan Medical University (approval no. 2024.39). Written informed consent was obtained from all participants prior to surgery.

Patient consent for publication

Not applicable.

Competing interests

The authors declare that they have no competing interests.

References

1. Sung H, Ferlay J, Siegel RL, Laversanne M, Soerjomataram I, Jemal A and Bray F: Global cancer statistics 2020: GLOBOCAN estimates of incidence and mortality worldwide for 36 cancers in 185 countries. CA Cancer J Clin 71: 209-249, 2021.
2. Majeed U, Manochakian R, Zhao Y and Lou Y: Targeted therapy in advanced non-small cell lung cancer: Current advances and future trends. J Hematol Oncol 14: 108, 2021.
3. Lu T, Yang X, Huang Y, Zhao M, Li M, Ma K, Yin J, Zhan C and Wang Q: Trends in the incidence, treatment and survival of patients with lung cancer in the last four decades. Cancer Manag Res 11: 943-953, 2019.
4. Gallinari P, Di Marco S, Jones P, Pallaoro M and Steinkühler C: HDACs, histone deacetylation and gene transcription: From molecular biology to cancer therapeutics. Cell Res 17: 195-211, 2007.
5. Seto E and Yoshida M: Erasers of histone acetylation: The histone deacetylase enzymes. Cold Spring Harb Perspect Biol 6: a018713, 2014.
6. Zhang LB, Bu L, Hu J, Xu ZY, Ruan LB, Fang Y and Wang P: HDAC1 knockdown inhibits invasion and induces apoptosis in non-small cell lung cancer cells. Biol Chem 399: 603-610, 2018.
7. Sasaki H, Moriyama S, Nakashima Y, Kobayashi Y, Kiriyama M, Fukai I, Yamakawa Y and Fujii Y: Histone deacetylase 1 mRNA expression in lung cancer. Lung Cancer 46: 171-178, 2004.
8. Cao LL, Song XX, Pei L, Liu LH, Wang H and Jia M: Histone deacetylase HDAC1 expression correlates with the progression and prognosis of lung cancer: A meta-analysis. Medicine (Baltimore) 96: e7663, 2017.

9. Minamiya Y, Ono T, Saito H, Takahashi N, Ito M, Mitsui M, Motoyama S and Ogawa J: Expression of histone deacetylase 1 correlates with a poor prognosis in patients with adenocarcinoma of the lung. Lung Cancer 74: 300-304, 2011.
10. Wang L, Li H, Ren Y, Zou S, Fang W, Jiang X, Jia L, Li M, Liu X, Yuan X, *et al*: Targeting HDAC with a novel inhibitor effectively reverses paclitaxel resistance in non-small cell lung cancer via multiple mechanisms. Cell Death Dis 7: e2063, 2016.
11. Lin YC, Lin YC, Shih JY, Huang WJ, Chao SW, Chang YL and Chen CC: DUSP1 expression induced by HDAC1 inhibition mediates gefitinib sensitivity in non-small cell lung cancers. Clin Cancer Res 21: 428-438, 2015.
12. Zhang LL, Li Q, Zhong DS, Zhang WJ, Sun XJ and Zhu Y: MCM5 aggravates the HDAC1-mediated malignant progression of lung cancer. Front Cell Dev Biol 9: 669132, 2021.
13. Fan Y, Ji X, Yuan K, Wu Q and Lou M: HDAC1 Mediates immunosuppression of the tumor microenvironment in non-small cell lung cancer. J Inflamm Res 18: 3333-3347, 2025.
14. Kong Y, Jiang R, Zhou H, Ge M, Lin H, Wang Y, Yao R, Wang Q, Liang X, Li J and Zhou X: PHF12 regulates HDAC1 to promote tumorigenesis via EGFR/AKT signaling pathway in non-small cell lung cancer. J Transl Med 22: 689, 2024.
15. Gui HX, Peng J, Yang ZP, Chen LY, Zeng H, Shao YT, Mu X, Hao Q, Yang Y, An S, *et al*: HDAC1-Smad3-mSin3A complex is required for Smad3-induced transcriptional inhibition of hepatocyte growth factor receptor in human lung cancers. Carcinogenesis 42: 587-600, 2021.
16. Amin MB, Edge SB, Greene FL, Byrd DR, Brookland RK, Washington MK, Gershenwald JE, Compton CC, Hess KR, Sullivan DC, *et al*: AJCC Cancer Staging Manual. (8th edition). Springer, New York, NY, 2017.
17. Liu E, Zhou Q, Xie AJ, Li X, Li M, Ye J, Li S, Ke D, Wang Q, Xu ZP, *et al*: Tau acetylates and stabilizes β-catenin thereby promoting cell survival. EMBO Rep 21: e48328, 2020.
18. You H, Li Q, Kong D, Liu X, Kong F, Zheng K and Tang R: The interaction of canonical Wnt/β-catenin signaling with protein lysine acetylation. Cell Mol Biol Lett 27: 7, 2022.
19. Huang X, Xu J, Huang M, Li J, Dai L, Dai K and Zhang X: Histone deacetylase1 promotes TGF-β1-mediated early chondrogenesis through down-regulating canonical Wnt signaling. Biochem Biophys Res Commun 453: 810-816, 2014.
20. Xu HT, Wang L, Lin D, Liu Y, Liu N, Yuan XM and Wang EH: Abnormal β-catenin and reduced axin expression are associated with poor differentiation and progression in non-small cell lung cancer. Am J Clin Pathol 125: 534-541, 2006.
21. He TC, Sparks AB, Rago C, Hermeking H, Zawel L, Da Costa LT, Morin PJ, Vogelstein B and Kinzler KW: Identification of c-MYC as a target of the APC pathway. Science 281: 1509-1512, 1998.
22. Shtutman M, Zhurinsky J, Simcha I, Albanese C, D'Amico M, Pestell R and Ben-Ze'ev A: The cyclin D1 gene is a target of the β-catenin/LEF-1 pathway. Proc Natl Acad Sci USA 96: 5522-5527, 1999.
23. Foltz G, Yoon JG, Lee H, Ma L, Tian Q, Hood L and Madan A: Epigenetic regulation of wnt pathway antagonists in human glioblastoma multiforme. Genes Cancer 1: 81-90, 2010.
24. West AC and Johnstone RW: New and emerging HDAC inhibitors for cancer treatment. J Clin Invest 124: 30-39, 2014.
25. Kumar R and Bashyam MD: Multiple oncogenic roles of nuclear beta-catenin. J Biosci 42: 695-707, 2017.
26. Nelson WJ and Nusse R: Convergence of Wnt, beta-catenin and cadherin pathways. Science 303: 1483-1487, 2004.
27. Valenta T, Hausmann G and Basler K: The many faces and functions of β-catenin. EMBO J 31: 2714-2736, 2012.
28. Maher MT, Mo R, Flozak AS, Peled ON and Gottardi CJ: Beta-catenin phosphorylated at serine 45 is spatially uncoupled from beta-catenin phosphorylated in the GSK3 domain: Implications for signaling. PLoS One 5: e10184, 2010.
29. MacDonald BT, Tamai K and He X: Wnt/beta-catenin signaling: Components, mechanisms and diseases. Dev Cell 17: 9-26, 2009.
30. Scrima M, De Marco C, Fabiani F, Franco R, Pirozzi G, Rocco G, Ravo M, Weisz A, Zoppi P, Ceccarelli M, *et al*: Signaling networks associated with AKT activation in non-small cell lung cancer (NSCLC): New insights on the role of phosphatydil-inositol-3 kinase. PLoS One 7: e30427, 2012.
31. Ciuffreda L, Cesta Incani U, Steelman LS, Abrams SL, Falcone I, Del Curatolo A, Chappell WH, Franklin RA, Vari S, Cognetti F, *et al*: Signaling intermediates (MAPK and PI3K) as therapeutic targets in NSCLC. Curr Pharm Des 20: 3944-3957, 2014.
32. Vicent S, López-Picazo JM, Toledo G, Lozano MD, Torre W, Garcia-Corchón C, Quero C, Soria JC, Martín-Algarra S, Manzano RG and Montuenga LM: ERK1/2 is activated in non-small-cell lung cancer and associated with advanced tumours. Br J Cancer 90: 1047-1052, 2004.
33. Han F, Chen S, Zhang K, Zhang K, Wang M and Wang P: Single-cell transcriptomic sequencing data reveal aberrant DNA methylation in SMAD3 promoter region in tumor-associated fibroblasts affecting molecular mechanism of radiosensitivity in non-small cell lung cancer. J Transl Med 22: 288, 2024.
34. Matsuura I, Wang G, He D and Liu F: Identification and characterization of ERK MAP kinase phosphorylation sites in Smad3. Biochemistry 44: 12546-12553, 2005.
35. Ma T, Yan B, Hu Y and Zhang Q: HOXA10 promotion of HDAC1 underpins the development of lung adenocarcinoma through the DNMT1-KLF4 axis. J Exp Clin Cancer Res 40: 71, 2021.
36. Jiang Z, Yang H, Zhang X, Wang Z, Rong R and Wang X: Histone deacetylase-1 as a prognostic factor and mediator of gastric cancer progression by enhancing glycolysis. Hum Pathol 85: 194-201, 2019.
37. Cao LL, Yue ZH, Liu LH, Pei L, Yin Y, Qin L, Zhao J, Liu HX, Wang H and Jia M: The expression of histone deacetylase HDAC1 correlates with the progression and prognosis of gastrointestinal malignancy. Oncotarget 8: 39241-39253, 2017.
38. Weichert W, Röske A, Niesporek S, Noske A, Buckendahl AC, Dietel M, Gekeler V, Boehm M, Beckers T and Denkert C: Class I histone deacetylase expression has independent prognostic impact in human colorectal cancer: Specific role of class I histone deacetylases in vitro and in vivo. Clin Cancer Res 14: 1669-1677, 2008.
39. Ishihama K, Yamakawa M, Semba S, Takeda H, Kawata S, Kimura S and Kimura W: Expression of HDAC1 and CBP/p300 in human colorectal carcinomas. J Clin Pathol 60: 1205-1210, 2007.
40. Witt AE, Lee CW, Lee TI, Azzam DJ, Wang B, Caslini C, Petrocca F, Grosso J, Jones M, Cohick EB, *et al*: Identification of a cancer stem cell-specific function for the histone deacetylases, HDAC1 and HDAC7, in breast and ovarian cancer. Oncogene 36: 1707-1720, 2017.
41. Rivas M, Johnston ME II, Gulati R, Kumbaji M, Aguiar TFM, Timchenko L, Krepischi A, Shin S, Bondoc A, Tiao G, *et al*: HDAC1-dependent repression of markers of hepatocytes and P21 is involved in development of pediatric liver cancer. Cell Mol Gastroenterol Hepatol 12: 669-682, 2021.
42. Xie J, Wang Z, Fan W, Liu Y, Liu F, Wan X, Liu M, Wang X, Zeng D, Wang Y, *et al*: Targeting cancer cell plasticity by HDAC inhibition to reverse EBV-induced dedifferentiation in nasopharyngeal carcinoma. Signal Transduct Target Ther 6: 333, 2021.